Reaction Kinetics Modeling and Thermal Properties of Epoxy–Amines as Measured by Modulated-Temperature DSC. II. Network-Forming DGEBA + MDA

Steven Swier, Guy Van Assche, Bruno Van Mele

Department of Physical Chemistry and Polymer Science, Vrije Universiteit Brussel (VUB), Pleinlaan 2, B-1050 Brussels, Belgium

Received 3 February 2003; accepted 29 July 2003

ABSTRACT: Reaction-induced vitrification takes place in the network-forming epoxy–amine system diglycidyl ether of bisphenol A (DGEBA) + methylenedianiline (MDA) when the glass-transition temperature (T_g) rises above the cure temperature (T_{cure}). This chemorheological transition results in diffusion-controlled reaction and can be followed simultaneously with the reaction rate in modulated-temperature DSC (MTDSC). To predict the effect of T_{cure} and the NH/epoxy molar mixing ratio (r) on the reaction rate in chemically controlled conditions, a mechanistic approach was used based on the nonreversing heat flow and heat capacity MTDSC signals, in which the reaction steps of primary (E_{1OH} = 44 kJ mol^{-1}) and secondary amine (E_{2OH} = 48 kJ mol^{-1}) with the epoxy–hydroxyl complex predominating. The diffusion factor DF as defined by the Rabinowitch approach expresses whether the chemical reaction rate or the diffusion rate determines the overall reaction rate. A model based on the free volume theory together with an Arrhenius temperature dependency was used to calculate the diffusion rate constant in DF as a function of conversion (x) and T_{cure}. The relation between x, r, and T_g, needed in this model, can be predicted with the Couchman equation. An experimental approximation for DF is the mobility factor DF* obtained from the heat capacity signal at a modulation frequency of 1/60 Hz, normalized for the effect of the reaction heat capacity in the liquid state and the change in C_p in the glassy region with x and T_{cure}. In this way, an optimized set of diffusion parameters was obtained that, together with the optimized kinetic parameters set, can predict the reaction rate for different cure schedules and for stoichiometric and off-stoichiometric mixtures. © 2004 Wiley Periodicals, Inc. J Appl Polym Sci 91: 2814–2833, 2004

Key words: modulated-temperature differential scanning calorimetry (MTDSC); step-growth polymerization; kinetics (polym.); modeling; thermosets

INTRODUCTION

During the curing of network-forming epoxy–amine systems crosslinking results in drastic property changes, which can have an impact on the reaction rate of the system. The reactive mixture with low glass-transition temperature (T_{g0}) is transformed into a polymeric glass having a glass-transition temperature (T_g) far above room temperature. Curing to maximum epoxy conversion involves a change in T_g from T_{g0} to T_{gfull}. Because network-forming epoxy–amine systems usually exhibit a high T_{gfull}, isothermal cure (at T_{cure}) is performed below this glass transition ($T_{cure} < T_{gfull}$).[1] While T_{cure} is above the increasing T_g, the reaction rate will be governed by the chemistry and concentration of the molecular species in the system (chemically controlled reaction). At a certain point in the reaction ($T_{cure} - T_g$) will become small, inhibiting the diffusion of reactive groups and drastically changing the overall reaction rate (diffusion-controlled reaction). In step-growth polymerization (epoxy–amine systems) the degree of polymerization increases steadily throughout the reaction (with a steep increase at the end), whereas the monomer is consumed in its early stages.[2] Because of the continuous size distribution of reactive species during the cure process, diffusion control is nonspecific and determined by chain segment mobility, which is essentially frozen in at vitrification when T_g reaches T_{cure}.[3]

Thus, for epoxy–amine cure, reaction-induced vitrification marks the onset of diffusion-controlled reaction. From this onset, the conversion rate predicted by chemical kinetics $(dx/dt)_{kin}$ has to be corrected with a diffusion factor (DF) to describe the experimentally measured conversion rate $(dx/dt)_{obs}$[4]:

$$\left[\frac{dx}{dt}(x, T)\right]_{obs} = \left[\frac{dx}{dt}(x, T)\right]_{kin} DF(x, T) \qquad (1)$$

where $(dx/dt)_{obs}$ is proportional to the heat flow from modulated-temperature differential scanning calorimetry (MTDSC) measurements[5] and x corresponds to

Correspondence to: B. Van Mele (bvmele@vub.ac.be).

Contract grant sponsor: Flemish Institute for the Promotion of Scientific-Technological Research in Industry (I.W.T.).

the *epoxy* conversion. DF will range from 1 in the undisturbed state with no mobility constraints to 0 in the frozen glass (below T_g). To quantify DF, the transition from chemically controlled to diffusion-controlled reaction can be described by the Rabinowitch equation, which is derived from the activated complex theory.[6,7] The time for the disappearance of a reactant is equal to the time for diffusion plus the time for chemical reaction leading to bond formation:

$$t_{\text{reaction}} = t_{\text{diffusion}} + t_{\text{chem kin}} \tag{2}$$

When the overall kinetic rate constant is termed k_{kin}, the following equation was derived for the diffusion factor[8]:

$$DF(x, T) = \frac{k_D(x, T)}{k_D(x, T) + k_{\text{kin}}(x, T)} \tag{3}$$

The rate constant for diffusion k_D can be determined from a model based on the free-volume concept and a description similar to the Williams–Landel–Ferry (WLF) equation.[8,9] The equations used for k_D together with the T_g–x relationship needed for its calculation is given below in the section on rate of diffusion.

Modeling approaches for the cure kinetics of these systems usually consider a semiempirical, explicit relationship between the conversion rate $[(dx/dt)_{\text{kin}}]$ and conversion (x) of epoxide groups.[8,10–13] Although the effect of T_{cure} on the cure kinetics of epoxy–amine systems can be predicted, a mechanistic approach must be used to extend the simulation capabilities to the effect of mixture composition and epoxy–amine chemistry.[14] This was previously illustrated for the epoxy–amine systems phenyl glycidyl ether (PGE) + aniline[14] and DGEBA + aniline (first part of this series),[15] leading to small molecules and linear macromolecules, respectively. A mechanistic model including both reactive and nonreactive complexes in combination with the amine–epoxy reaction steps adequately predicted MTDSC profiles for nonreversing heat flow and heat capacity and concentration evolutions obtained from chromatographic or spectroscopic techniques. Chemically controlled reaction occurred in both systems at the usual cure temperatures investigated. A few studies used a mechanistic approach including a diffusion-controlled reaction. In such studies, every reaction step was corrected with the same diffusion factor, a correction permitted in view of the step-growth polymerization mechanism of epoxy–amine systems.[16–18]

MTDSC can be used to study cure and vitrification simultaneously in the nonreversing heat flow and heat capacity signal (C_p), respectively, as was shown for different network-forming epoxy–amine and epoxy–anhydride systems.[19–23] At high conversions, where the reaction mixture is insoluble and analysis by spectroscopic techniques such as FTIR and NMR becomes ineffective, the heat capacity is still very sensitive to vitrification. Although other dynamic techniques like dielectric spectroscopy, dynamic mechanical thermal analysis, and dynamic rheometry are also adequately able to detect vitrification, they are not suited to detect the conversion development simultaneously.[24–27] Moreover, C_p is able to resolve the primary and secondary amine–epoxy reaction steps in the chemically controlled regime.[5,14,15]

The loss of (cooperative) mobility attributed to vitrification can be quantified by defining a mobility factor DF*[8,19–21]:

$$\text{DF}^*(x, T) = \frac{C_p(x, T) - C_{\text{pg}}(x, T)}{C_{\text{pl}}(x, T) - C_{\text{pg}}(x, T)} \tag{4}$$

This factor changes from unity for the liquid, with heat capacity C_{pl}, to zero for a frozen glassy state, with heat capacity C_{pg}, at the same conversion and temperature. For epoxy–amine systems, DF* turns out to almost coincide with DF when measured with a modulation frequency (f_M) of 1/60 Hz.[8,21,22,28] This means that in these systems the characteristic time scale for the rate-determining mobility upon transition to the diffusion-controlled reaction corresponds to the time scale involved in the glass-transition region measured in these modulation conditions ($\sim 10^1$–10^2 s in MTDSC). Thus, not the center-of-mass diffusion but the diffusion of chain segments is important in diffusion-controlled epoxy–amine reactions. Because the reaction rate itself depends on the cure temperature and is unaffected by the imposed modulation frequency, care must be taken when comparing the mobility factor obtained at f_M different from 1/60 Hz, termed MF(f_M), with DF, corresponding to a characteristic frequency f^*.[8,28] Corrections to the T_g–x equation are needed to include experimental MF(f_M) profiles, as discussed below in the section on rate of diffusion.[8] The currently available frequency range of 0.01–0.05 Hz (modulation periods of 100 to 20 s), however, is restricted for investigation of this frequency effect. By using light (heating) modulated DSC and complex sawtooth modulation the frequency range has been extended to the higher (1 Hz) and lower limits (0.002 Hz), respectively.[29]

Note that the use of the mobility factor as an experimental measure of the diffusion factor cannot be extended to all reacting (polymeric) systems. In free-radical polymerization, reaction steps like propagation and termination are affected in a different way by a decrease in mobility as determined from the heat capacity signal (specific diffusion control).[30,31] On the other hand, the reaction rate during the formation of an inorganic polymer glass is nearly uninfluenced by the vitrification process.[19,30]

Because the useful cure temperature range lies far below the full cure glass-transition temperature ($T_{g\text{full}}$ = 175°C for a stoichiometric mixture) in the case of the network-forming system DGEBA + methylenedianiline (MDA) used in this work, the incorporation of diffusion restrictions in the mechanistic reaction model will be required. Both the nonreversing heat flow and heat capacity signals from MTDSC will be quantified to provide information about the chemically controlled and diffusion-controlled reaction and will subsequently be used as input signals for this model. Apart from the effect of T_{cure} and mixture composition, the influence of the modulation frequency will also be addressed.

EXPERIMENTAL

Materials

A high-purity bifunctional epoxy diglycidyl ether of bisphenol A (DGEBA), under the trade name Epon™ Resin 825 from Shell (Houston, TX), was used (epoxy equivalent weight = 180 g/mol).[32] A single molecular structure was reported. Methylenedianiline (MDA, f = 4, M_w = 198 g mol^{-1}, purity = 99%, T_M = 90°C) was provided by Aldrich (Bornem, Belgium). Appropriate amounts of DGEBA and MDA (mixture composition: r = mol NH/mol epoxide) were mixed with a mechanical mixer at 80°C for 5 min. A negligible amount of reaction occurred in these mixing conditions.

Modulated-temperature DSC

A TA Instruments 2920 DSC (TA Instruments, New Castle, DE) with MDSC™ option and a refrigerated cooling system (RCS) was used for the MTDSC cure experiments. Samples ranging from 5 to 10 mg were measured using hermetic crucibles. Helium was used as a purge gas (25 mL/min). Indium and cyclohexane were used for temperature and enthalpy calibration. Heat capacity calibration was performed with a poly(methyl methacrylate) (PMMA) standard (supplied by Acros, Geel, Belgium), using the heat capacity difference between two temperatures (one above and one below the glass-transition temperature of PMMA[33]) to ensure that heat capacity changes were adequately measured. Quasi-isothermal measurements of the reaction enthalpy and heat capacity were performed using a modulation amplitude of 1°C in combination with a period of 60 s.

A TA Instruments Q1000 with an RCS cooling unit was used to determine the frequency dependency of the heat capacity evolution.[34] The Q1000 DSC cell uses Tzero™ technology. This new cell design allows for balancing of thermal resistance, thermal capacitance, mass, and heating rate differences between the sample and reference sides.[35] Moreover, thermal resistance between sensor and pans and pan mass is also included in the heat flow equations. Nitrogen was used as a purge gas (25 mL/min), and hermetic crucibles were used with samples ranging from 5 to 10 mg. The heat capacity signal was calibrated for the effect of temperature amplitude (A_T) and modulation frequency (f_M). Although no correction was needed for A_T ranging from 0.1 to 1°C, corrections in C_p of up to 40% were required when f_M was chosen between 1/40 and 1/10 Hz (full f_M range in Tzero from 0.1 to 0.005 Hz).

RESULTS AND DISCUSSION

Model for reaction kinetics including diffusion effects

Reaction mechanism

The reaction of primary and secondary amine functionalities with an epoxy–hydroxyl complex predominates the reaction kinetics of DGEBA + aniline.[15] Initiation of the reaction occurs between the primary amine and the epoxy–amine complex. This reaction mechanism was also confirmed for the model epoxy–amine system phenyl glycidyl ether (PGE) + aniline in which only low molecular weight compounds are formed.[14] Equilibrium complexes between groups of the reagents and products (epoxy, amines, hydroxyl, and ether groups) must be included to obtain adequate simulations of experimental trends at different T_{cure} and mixture composition r. Details about the notation used for chemical species, rate constants, and equilibrium constants can be found in Swier and Van Mele.[14,15]

To account for diffusion effects in the reaction kinetics model, an expression for the overall kinetic rate constant k_{kin} is required [see eq. (3)]. The concentration and consumption rate of epoxide groups as calculated in the program FITME from the rate constants in the reaction mechanism will be used for this purpose (in s^{-1}):

$$k_{\text{kin}}(x, T) = -\frac{d[\text{E}]/dt}{[\text{E}]}(x, T) \tag{5}$$

where $-d[\text{E}]/dt$ is the global consumption rate of epoxide groups (in mol kg^{-1} s^{-1}) and [E] is the concentration of epoxide groups (in mol kg^{-1}).

Rate of diffusion

The diffusion rate constant k_D can be expressed in terms of the overall diffusion coefficient D[9,36]:

$$k_D = k_{D0}(T)D(x, T) \tag{6}$$

where $k_{D0}(T)$ is related to local conditions for the creation of the chemical bond.

In the case of step-growth polymerization, the diffusion of reactive groups is determined by the diffusion of chain segments. Therefore, D is expected to be inversely proportional to the relaxation time of polymer segments and can be expressed using a WLF-like equation.[37] Finally, by introducing an Arrhenius temperature dependency for $k_{D0}(T)$, k_D is given by[8]

$$\ln k_D(x, T) = \ln A_D - \frac{E_D}{RT} + \frac{C_1[T - T_g(x)]}{C_2 + T - T_g(x)} \quad (7)$$

where A_D is the preexponential factor and E_D is the activation energy for the diffusion rate constant k_{D0}; C_1 and C_2 are constants from the WLF equation characteristic for specific polymer systems.[38] For a fully cured stoichiometric DGEBA + MDA system, values for C_1 of 10.9 and for C_2 of 34.8°C were obtained from dynamic mechanical analysis.[39]

For network-forming systems, relationships between T_g and x can be subdivided into those that require the knowledge of the changing structural features of the molecular architecture (e.g., molecular weight, gel point, crosslink density, and onset of non-Gaussian behavior) and those that are based on thermodynamic considerations. The structural models attribute changes in T_g in the sol fraction to the drop in chain-end concentration as the molecular weight of the growing epoxy–amine chain increases and those in the gel fraction to further restriction to movement by the formation of branch points and crosslinks.[40,41] Especially in the case of off-stoichiometric compositions, these models are difficult to implement because structural features of the molecular architecture are difficult to obtain experimentally.[42,43]

An equation based on the Couchman approach for polymer blends has the potential of predicting T_g–x for different epoxy–amine chemistries and mixture compositions, while using only the thermal properties of the unreacted (subscript 0) and fully reacted (subscript full) material as input parameters.[44,45] As elaborated in the first part of this series,[15] a fitting parameter λ must be included; however, because the assumptions made for polymer blends are not valid during step-growth polymerization of epoxy–amines:

$$\ln T_g(x) = \frac{(x_{\text{full}} - x)\ln(T_{g0}) + \lambda \dfrac{\Delta C_{p\text{full}}}{\Delta C_{p0}} x \ln(T_{g\text{full}})}{(x_{\text{full}} - x) + \lambda \dfrac{\Delta C_{p\text{full}}}{\Delta C_{p0}} x} \quad (8)$$

where ΔC_{p0} and $\Delta C_{p\text{full}}$ are the heat capacity changes at T_{g0} and $T_{g\text{full}}$, respectively; x is the epoxy conversion. x_{full} designates the maximum attainable epoxy conversion: given that complete consumption of epoxide groups can be achieved for stoichiometric and excess amine mixtures, $x_{\text{full}} = 1$, whereas x_{full} will be <1 for systems with an excess in epoxide groups (see also the section on glass transition).

Finally, when the mobility factor is obtained at a frequency f_M different from the "characteristic frequency" f^*, the shift in T_g with modulation frequency f_M must be included in the T_g–x relationship[8]:

$$T_g(x, f_M) = T_g(x) + b \log \frac{f_M}{f^*} \quad (9)$$

where f^* is the characteristic frequency of the cooperative mobility frozen in at T_g and b is approximately 3–4°C. By using eq. (9), the mobility factor measured at another frequency, MF(f_M), can still be calculated from eqs. (3) and (7). Because DF is modeled with $f_M = f^*$, the information from experiments performed at different frequencies can be combined.

In summary, a diffusion-controlled reaction is included in this work by calculating DF [eq. (3)] from k_{kin} [eq. (5)] and k_D [eqs. (6)–(9)]. Taking into account the nature of step-growth polymerization with overall diffusion control, this single diffusion factor is then applied to every reaction step of the reaction mechanism (see Swier and Van Mele[15]).

Thermal properties as a function of x, r, and f_M

Details about the methodology used to determine T_g, x, $\Delta C_p(T_g)$, and the width of the glass-transition region (ΔT_g) for the DGEBA + MDA system can be found in the first part of this series.[15] The T_g–x–r relationship was used to calculate the diffusion rate constant k_D [eqs. (7) and (8)], whereas the evolutions of C_{pg} and C_{pl} with x are of interest in the determination of the mobility factor DF* [eq. (4)] (see also the section on methodology to obtain the mobility factor in isothermal and nonisothermal conditions). Note that for both stoichiometric and off-stoichiometric mixtures, x will designate the *epoxy* conversion.

Glass transition

Full cure glass transition ($T_{g\text{full}}$) *as a function of* r. To obtain the $T_{g\text{full}}$ of DGEBA + MDA as a function of r, nonisothermal cure experiments were performed at 2.5°C/min until reaction completion. The reaction enthalpy per mole of minority component was around -104 kJ mol^{-1} for all values of r, confirming full cure conditions.[46] The maximum $T_{g\text{full}}$ was found for the stoichiometric composition as shown in Figure 1 and as confirmed in the literature.[47–49] Residual unreacted groups in the off-stoichiometric mixtures can be thought of as plasticizers for the network, thus reducing T_g. However, the lower attainable crosslink density X_c is considered to be the determining factor in lowering T_g because crosslinks constitute the most

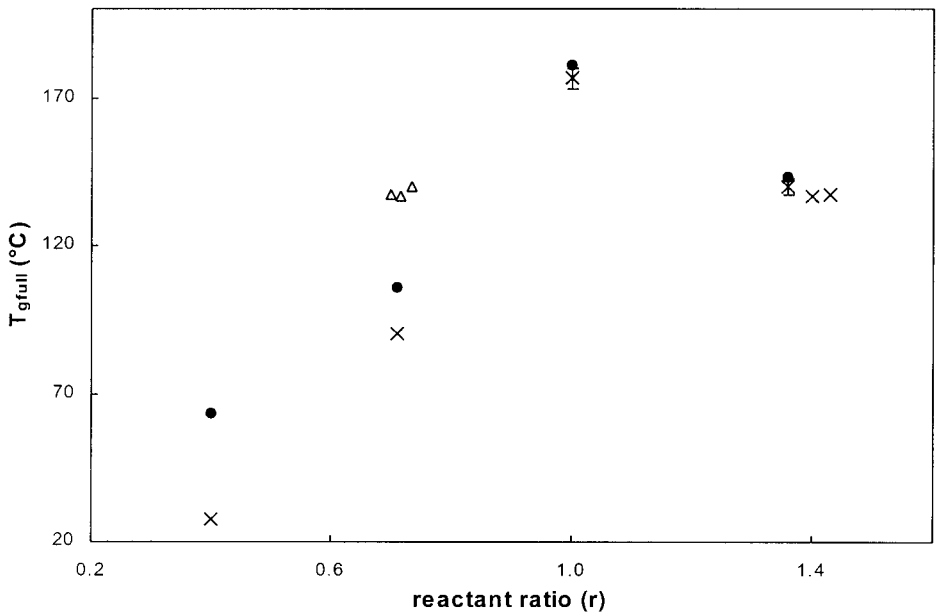

Figure 1 T_{gfull} as a function of reactant ratio (r) for DGEBA + MDA cured nonisothermally at 2.5°C/min until reaction completion (maximum end temperature of 230°C) (×); redefined reaction ratio ($r' = 1/r$) for $r > 1$ (△); T_g as determined after a subsequent nonisothermal cure at 1°C/min until 280°C is also shown (●).

immobile fragments of networks.[48] This can be confirmed by redefining the reactant ratio ($r' = 1/r$) for excess amine mixtures to be ≤ 1 (Δ). The T_{gfull} of these mixtures is higher than that of the excess epoxy mixtures and can be ascribed to a higher attainable X_c for a higher initial content of the tetrafunctional MDA hardener. Note that for the DGEBA + aniline system, the T_{gfull}–r and T_{gfull}–r' evolutions are found to coincide because both components are bifunctional and lead to a linear macromolecule without crosslinks (see first part of this series[15]).

When an additional nonisothermal cure was performed at 1°C/min up to 280°C, T_g increased slightly for the stoichiometric and excess amine mixtures, whereas the T_g of the excess epoxy mixtures increased significantly. Considering the high connectivity of the network, unreacted amine and epoxide groups are not necessarily closest neighbors and thus cannot meet and react with each other under normal reaction conditions. This was illustrated by a computer simulation of the network topology, indicating that a conversion of 95% can be reached.[48] A subsequent cure to 280°C seems to provide the circumstances for additional epoxy–amine reaction.

The significant T_g increase for mixtures with an excess in epoxide groups could be related to side reactions like homopolymerization or etherification, which occur at high cure temperatures.[50] However, these reactions are slow because the formed tertiary aromatic amine has little or no catalytic effect on the reaction.[18] In addition, reactions of thermal and thermooxidative degradation become important at temperatures > 200°C.[46] A nonisothermal MTDSC experiment was performed on a fresh mixture of the highest epoxy excess ($r = 0.4$) revealing a small extra, exothermic peak at 220°C (not shown). If the amine–epoxy reaction and the side reactions (homopolymerization or etherification) would occur to completion, the reaction enthalpy (ΔH_r) normalized per mole of epoxide groups would be around -100 kJ mol^{-1}.[5] Because the shoulder amounts to only -3 kJ mol^{-1}, a much smaller ΔH_r value of -47 kJ mol^{-1} was found. Degradation reactions are thus probably responsible for the additional peak. To avoid these reactions, T_{gfull} as obtained in moderate reaction conditions (heating at 2.5°C/min until amine–epoxy reaction completion) were used in this work.

T_g *as a function of* x *and* r. The relation between T_g and x provides the link between reaction kinetics in chemical control and *chemorheological* changes at a certain cure temperature, resulting in the diffusion-controlled reaction.[51] T_g–x relationships for three DGEBA + MDA mixture compositions were constructed by combining isothermal and nonisothermal cure schedules using moderate cure conditions to avoid side reactions (Fig. 2). The initial increase in T_g can be attributed to the drop in chain-end concentration in the sol fraction, whereas the subsequent faster increase results from the formation of branch points and crosslinks in the gel fraction.[40,41] The fact that T_g increases faster at high conversions makes it more sensitive for monitoring the extent of cure at higher extents of reaction than chemical conversion itself. Whereas the maximum T_{gfull} was found for the stoichiometric system, the highest T_g at

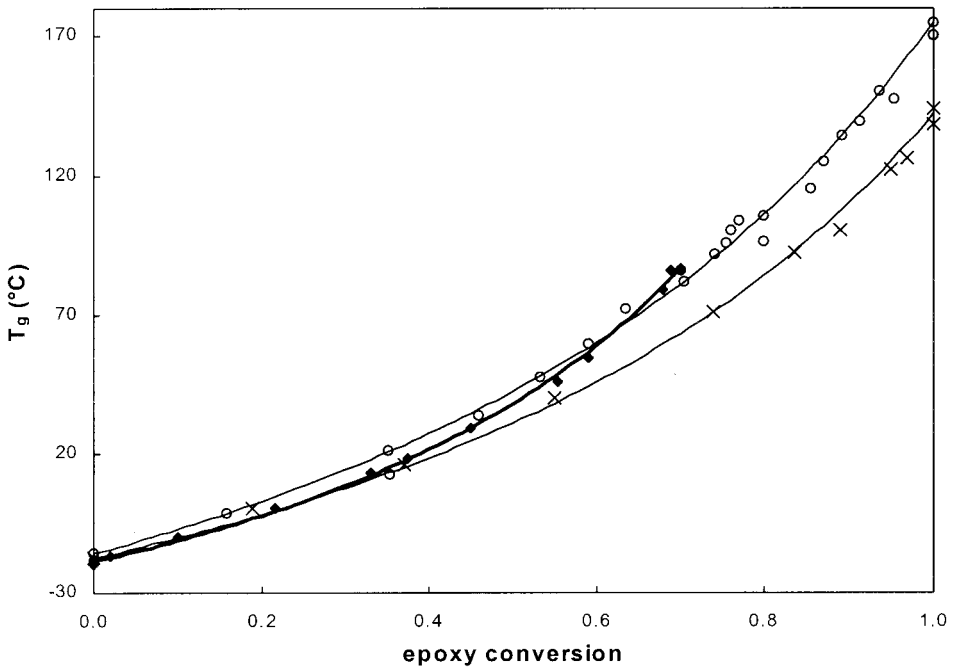

Figure 2 Glass-transition temperature (T_g) as a function of x for DGEBA + MDA mixtures with different mixture compositions: $r < 1$ (◆), $r = 1$ (○), and $r > 1$ (×); both isothermal and nonisothermal cure schedules were combined to obtain the entire conversion range, while ensuring moderate curing conditions to avoid side reactions; corrected Couchman relationship using the respective values of T_{g0}, $T_{g\text{full}}$, $\Delta C_{p\text{full}}/\Delta C_{p0}$, and best-fit values of λ (Table I) (thin lines for $r = 1$ and $r > 1$; thick line for $r < 1$).

70% conversion was found for the excess epoxy system, suggesting a higher crosslink density X_c at this point. In contrast, chain flexibility will increase with increasing epoxy content (note ether groups in DGEBA). By using a mixture of amines as the hardener, X_c was changed without alteration of the chain flexibility, showing that the former was the prominent factor in determining T_g.[52]

The T_g–x relation of eq. (8) was fitted to the experimental data in Figure 2. For the stoichiometric and excess amine system, the deviation from the Couchman equation is negligible ($\lambda \cong 1$, Table I). This means that in these cases, only thermal properties (T_g and ΔC_p) of the unreacted and fully reacted material are needed to predict the relation between T_g and x. This is confirmed by another study in which different reacting systems were analyzed with the Couchman equation.[45] A larger deviation was found, however, for the excess epoxy system ($\lambda = 0.73$).

TABLE I
Glass Transition of Unreacted (T_{g0} in K) and Fully Reacted ($T_{g\text{full}}$ in K) DGEBA + MDA Systems with Different Reactant Ratios (r)[a]

r	T_{g0}	$T_{g\text{full}}$	$\Delta C_{p\text{full}}/\Delta C_{p0}$	λ
0.7	254	364	0.75	0.73
1.0	257	448	0.58	1.00
1.36	256	413	0.59	0.95

[a] The experiment $\Delta C_{p\text{full}}/\Delta C_{p0}$ ratio is given together with the values for λ as obtained from the best fit to eq. (8).

The effect of f_M on T_g was considered by measuring T_{g0} of a stoichiometric DGEBA + MDA mixture. To obtain an extended frequency range, Tzero™ technology was used (f_M potentially in the range 0.005–0.1 Hz; see also experimental section). An increase in T_{g0} of 4.2°C (b) per decade was found.

ΔC_p at T_g as a function of x and r

The decrease of the heat capacity in the glassy state C_{pg} with x (Fig. 3) combined with the increase in the liquid state C_{pl} with x, attributed to the positive reaction heat capacity, would result in an increasing $\Delta C_p(T_g)$ with x. The greater temperature dependency of the C_p of the glassy state (below T_g) compared to that of the liquid state (above T_g), however, results in the measured decrease of $\Delta C_p(T_g)$ with x (Fig. 4). Note that the plateau to around 20% conversion is an indicator of the initial competition between both effects. The decreasing trend was also found for other epoxy resins and is attributed to the reduced configurational entropy of the more crosslinked systems (increase in X_c) with increasing x.[53–55] Following the fragility approach of Angell for nonpolymeric materials,[56] a transition to stronger structures was found during cure.

At full cure, $\Delta C_p(T_g)$ is 0.42, 0.32, and 0.28 J g^{-1} K^{-1} for r values of 0.7, 1.36, and 1.00, respectively. Indeed,

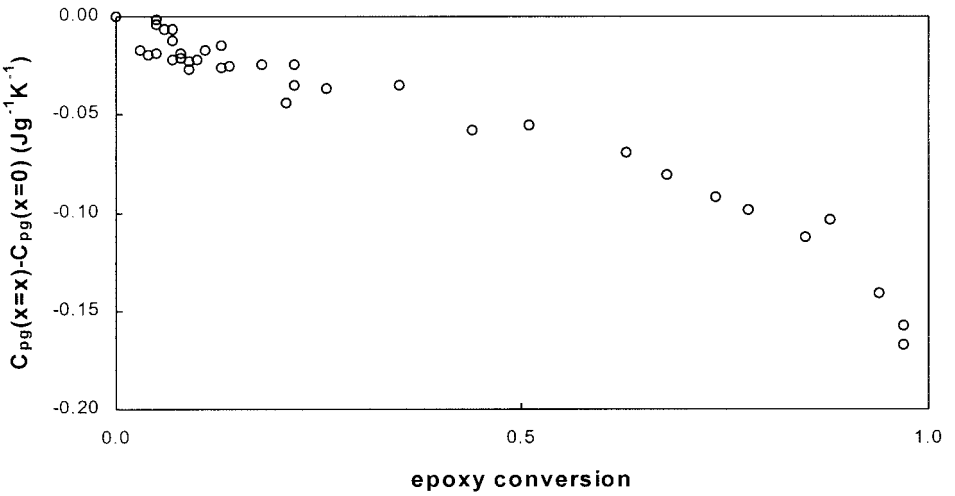

Figure 3 Difference between the heat capacity in the glassy state for the stoichiometric DGEBA + MDA mixture after a certain conversion [$C_{pg}(x = x)$] and for a fresh mixture [$C_{pg}(x = 0)$] as a function of x (note that x was obtained from the T_g measured in this experiment; see also Ref. 15).

the highest X_c is expected for the stoichiometric mixture, as confirmed by a study where the reactant ratio was changed over a much wider range.[48]

ΔT_g *as a function of* x *and* r. As stated for the linearly polymerizing DGEBA + aniline system, the broadening of the molecular weight distribution increases ΔT_g (Fig. 5). Two effects can be stated in the network system for the decrease in ΔT_g at high conversions: a decrease in concentration of unreacted functional groups and an increase in X_c. No unreacted groups remain in the stoichiometric system (Fig. 5, ○), which also has the highest X_c at reaction completion, clearly showing a decrease in ΔT_g starting from a conversion of 90%. Both the remaining unreacted groups and the lower crosslink density of the excess epoxy system (Fig. 5, ◆) are probably responsible for the absence of the maximum in this system. Note that ΔT_g is difficult to obtain over the entire conversion range for the

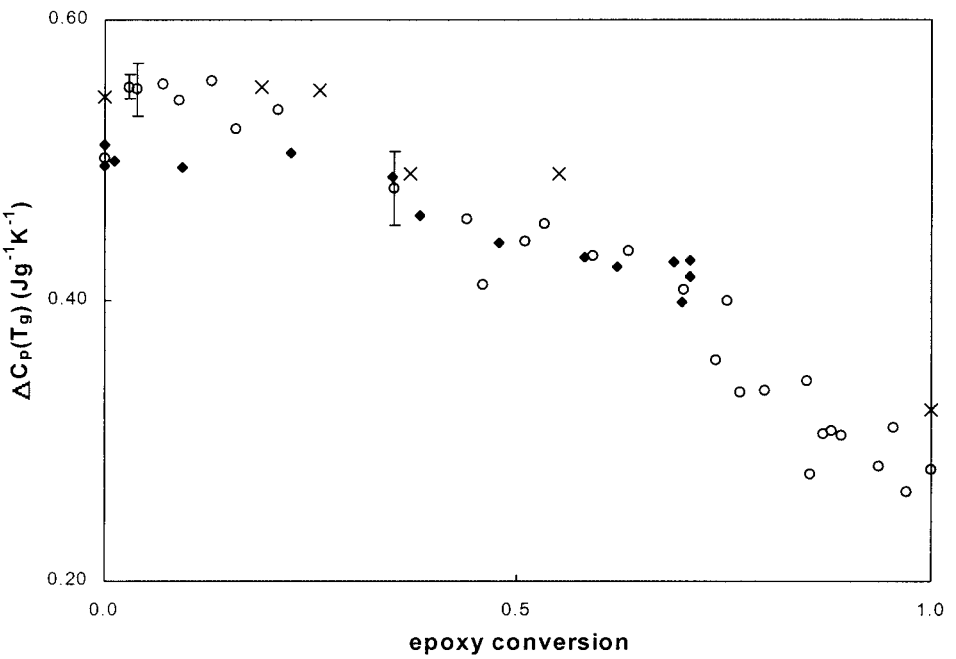

Figure 4 Heat cpacity change at T_g [$\Delta C_p(T_g)$] as a function of x as obtained from the heat capacity signal of MTDSC in nonisothermal experiments (note that x was obtained from the T_g measured in this experiment; see also Ref. 15); DGEBA + MDA mixtures with r values of 1.0 (○), 1.36 (×), and 0.7 (◆) are shown; error bars are included when more than two measurements were averaged.

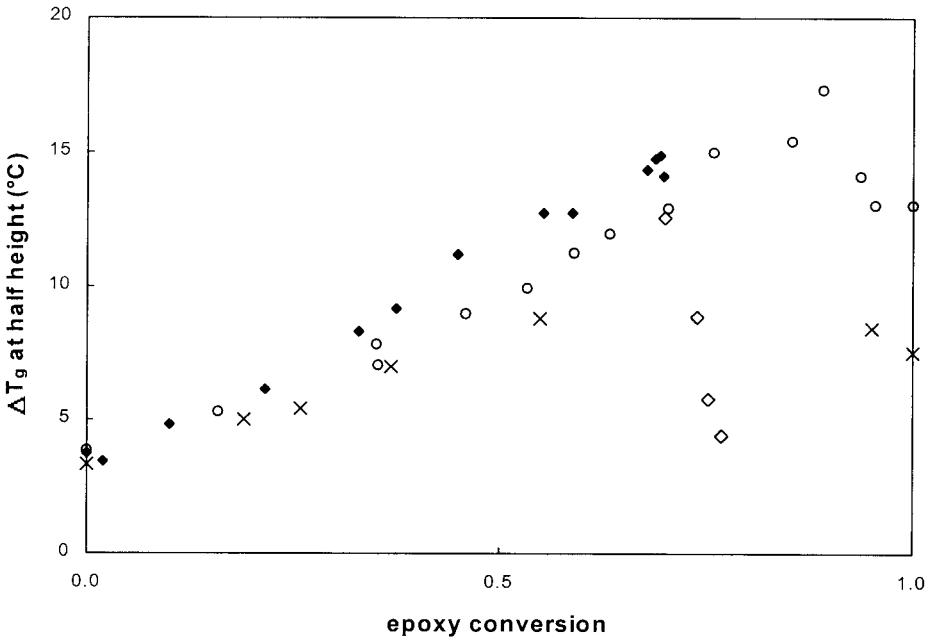

Figure 5 Width of glass-transition region ΔT_g, defined at the half-height of the derivative of the heat capacity signal in nonisothermal conditions, as a function of conversion for mixtures of DGEBA + MDA with a reactant ratio of 0.7 (◆), 1.0 (○), and 1.36 (×); values for stoichiometric DGEBA + MDA mixtures cured at 80°C in the diffusion-controlled vitrification region (cure time > 125 min) are also shown (◇).

excess amine system because vitrification (decrease in C_p) immediately follows the devitrification of a partially cured sample under nonisothermal conditions (not shown). This interferes with the characterization of the glass transition of the system formed in the preceding cure step.

The evolution of ΔT_g for the stoichiometric system cured at 80°C in the diffusion-controlled region (from $x = 70\%$, after 125 min at 80°C; see also Fig. 7, below) is also shown in Figure 5 (◇). An increase in T_g from 82°C ($x = 71\%$) to 104°C ($x = 77\%$) was still obtained, again indicating the sensitivity of T_g as a measure for x at high reaction extents.

The sharp drop in ΔT_g can be ascribed to the fact that, with increasing time or conversion in the diffusion-controlled region, a higher fraction of the material becomes frozen in. Further reaction of the fraction that is still mobile will increase its T_g and result in the narrower glass-transition region.

Simulation of concentration profiles

Indications about the differences in X_c can be obtained from simulated concentration profiles. Figure 6 depicts concentration profiles of secondary amines (A_2) and tertiary amines (A_3) as a function of the epoxy conversion, using an excess epoxy (E), stoichiometric, and excess amine mixture as simulated by the reaction kinetics model (discussed in the following section). When a higher initial concentration of A_1 is used, the primary amine–epoxy reaction step will be promoted, resulting in a higher intermediate concentration of A_2 and a lower concentration of A_3 at the same epoxy conversion.

At reaction completion, the stoichiometric system has the highest A_3 concentration, corresponding to the highest X_c, as was also suggested by the T_g–x relationships discussed in the section on glass transition, above. At reaction completion of the excess epoxy system (70%), however, A_3 is the highest for this system.

Optimization of the reaction kinetics model

Initial parameter set

Chemically controlled reaction. The optimized parameter set for rate constants and equilibrium constants obtained for DGEBA + aniline[15] will be used as an initial set to describe the reaction kinetics for DGEBA + MDA in the chemically controlled region (see also Table III).

Diffusion-controlled reaction. To obtain an initial set of parameters for the diffusion-controlled reaction, k_D [eq. (7)] can be determined as a function of the isothermal cure temperature T_{cure}, x, and r, following an approach proposed in Van Assche,[8] Van Hemelrijck,[57] and Van Mele et al.[58] An assumption of this method is that the mobility factor DF* can be used as an experimental approximation for the diffusion factor DF (de-

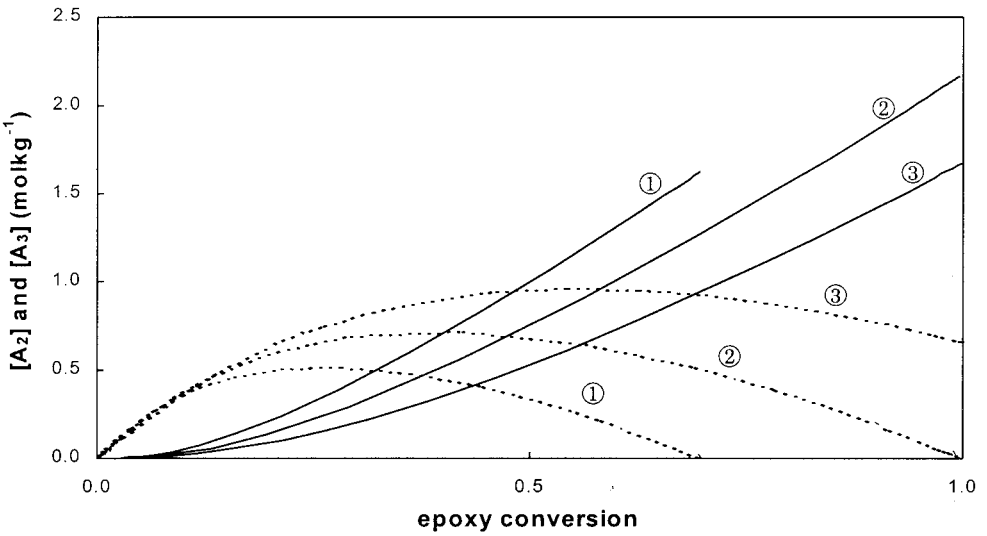

Figure 6 Simulation of the concentration profiles of secondary amines (A_2, dashed line) and tertiary amine groups (A_3, line) as a function of the epoxy conversion for the nonisothermal cure at 2.5°C/min of three mixture compositions: $r = 0.7$ (①), $r = 1.0$ (②), and $r = 1.36$ (③).

scribing the influence of overall diffusion control for step-growth polymerization). In this way, k_D can be calculated from eq. (3) and from an estimate for the overall kinetic rate constant k_{kin}. The diffusion parameters, as defined in eq. (7), are summarized in Table II for a stoichiometric and excess amine DGEBA + MDA mixture.

Optimized set of parameters for chemically controlled reactions

To obtain parameters for the reaction kinetics in chemically controlled conditions, the nonreversing heat flow and heat capacity signals were used before the occurrence of reaction-induced vitrification. The onset in the relaxation peak of the heat flow phase is a sensitive probe in this respect[21] (see also Fig. 7, below). The link between the MTDSC signals and the concentration profiles was previously discussed.[15]

Experiments in a wide range of cure temperatures (50–120°C) were used for reactant ratios r of 0.7, 1.0, and 1.36. Nonisothermal measurements with heating rates of 0.2, 1, and 2.5°C/min were also provided as input for the optimization. The resulting set of kinetic and equilibrium parameters and parameters for the prediction of the heat capacity change is given in Table III. The activation energies of the amine–epoxy reactions catalyzed by hydroxyl groups correspond to values found for DGEBA + MDA from empirical approaches.[59]

The optimized parameter set for the DGEBA + aniline system[15] is also included in Table III. A comparison between both epoxy–amine systems will be given after including the diffusion-controlled reaction for the DGEBA + MDA system (see the section on optimized set of diffusion parameters, below).

TABLE II
Diffusion Parameters from Eq. (7)[a]

r	$\ln A_D$	E_D (kJ mol^{-1})	C_1	T_{cure} range (°C)
1.0	12.3	53.1	6 ± 1	70–120
1.36	13.4	53.7	7 ± 2	50–110

[a] Determined from the approach discussed in Refs. 8, 57, and 58 (see text); C_2 was taken to be equal to the universal value from the WLF approach: $C_2 = 51.6$°C.

Methodology to obtain the mobility factor in isothermal and nonisothermal conditions

Isothermal cure. The simulation of the nonreversing heat flow and heat capacity change during the chemically controlled isothermal cure of stoichiometric DGEBA + MDA mixtures is shown in Figure 7 (thick line). Note that all MTDSC experiments were performed with a f_M equal to 1/60 Hz. Because all depicted cure temperatures are below T_{gfull} for this mixture composition (175°C, see Fig. 2), reaction-induced vitrification will occur at a certain conversion along this cure path. This transition from a rubbery to a glassy material can be detected as the onset of the relaxation peak in the heat flow phase signal (Fig. 7, ●).[21] An additional upward peak is present in this signal for the highest cure temperature (100°C, ~ 40 min) and has been attributed to a contribution of the reaction rate.[28,57] This effect will not be exploited in this work because the nonreversing heat flow is much more reliable for a quantitative measurement of the reaction rate in a wide range of cure temperatures.

TABLE III
Optimized Set of Parameters to Describe the Chemically Controlled Reaction of DGEBA + MDA[a]

Kinetic parameters (kg mol^{-1} s^{-1})						Equilibrium constant K_i (kg mol^{-1})					$\Delta_r C_p$ (J mol^{-1}K^{-1})
k_{1A1}		k_{1OH}		k_{2OH}							
E_{1A1}	log A_{1A1}	E_{1OH}	log A_{1OH}	E_{2OH}	log A_{2OH}	EOH	A1OH	EA1	EtOH	EtA1	a/b
7.58	7.4	44.0	3.9	48.3	4.2	0.45	0.16	0.18	0.79	0.17	18.0/19.6
Parameters obtained for DGEBA + aniline											
79.6	7.5	48.0	4.4	48.4	4.1	0.20	0.50	0.18	0.55	0.18	18.0/19.6

[a] Kinetic (k) and equilibrium (K) parameter set and $\Delta_t C_p$ parameters a and b [from eq. (4) in Ref. 15]; the parameters for the DGEBA + aniline system are given for comparison; activation energies (E) are in kJ mol^{-1}; preexponential factors (A) are in kg mol^{-1} s^{-1}.

The agreement between simulation and experiment is satisfactory in the chemically controlled region, whereas the retardation of the reaction in the diffusion-controlled region can be clearly distinguished (compare thin line of simulation with experimental nonreversing heat flow). The conversion reached after cure at 100, 80, and 70°C is 88, 81, and 77%, respectively (see also Fig. 8), corresponding to a final T_g of 130, 109, and 97°C, respectively. In comparison to the onset of vitrification, an additional reaction advancement of about 10%, together with an increase of about 30°C in T_g, occurs in all diffusion-controlled conditions. Thus, this region should not be overlooked when designing cure schedules for epoxy–amine systems.

To obtain the mobility factor, as defined in eq. (4), the reference heat capacity evolutions in both the liquid state [$C_{pl}(x, T_{cure})$] and the glassy state [$C_{pg}(x, T_{cure})$] are required. The former can be obtained from the simulated heat capacity change (thin line in Fig. 7). By expressing C_{pl} as a function of conversion (not shown) and by using the conversion as obtained from the nonreversing heat flow, $C_{pl}(x, T_{cure})$ was calculated and plotted as a function of cure time (dashed line in Fig. 7). The glassy state reference heat capacity was obtained from Figure 3. Because T_{cure} is below the glass-transition region for all isothermal experiments, the final points in the heat capacity change signal correspond to complete vitrification.

The mobility factor DF* [= MF(f^*)] can then be calculated from the observed heat capacity evolution as depicted in Figure 8.

Effect of modulation frequency. To study the effect of f_M on the evolution of the mobility factor MF(f_M), a low cure temperature was selected (T_{cure} = 60°C). In this way, f_M can be changed *during* the cure experiment, while enough points can still be collected in the transition region of MF from one to zero. This procedure is preferable to using a series of separate cure experiments with one f_M because it avoids variations of the vitrification time arising from small changes in reactive mixtures (mixture composition, sample weight, sample to pan contact) and pan shapes (pan to sensor contact resistance). As can be seen in Figure 9, decreasing f_M results in a delay of vitrification because T_g interferes with T_{cure} at a higher conversion. Note that a lower temperature amplitude had to be used in the case of a higher f_M to ensure uniform heating and cooling of the sample within a modulation cycle (see also experimental section).

Because the reaction rate itself depends on the average cure temperature (60°C), the onset of diffusion-controlled reaction will remain at the same conversion. Thus, the diffusion factor DF will be unaffected by f_M. DF can be calculated according to eq. (1) from the ratio of the experimental heat flow and the one simulated in chemically controlled conditions (with the kinetic parameters from Table III). Figure 9 shows that DF is close to MF at a frequency around 1/60 Hz. By using MF at another f_M as a model for DF, an error would be made in determining the conversion at the onset of diffusion-controlled reaction: x changes by 4% for a change in f_M from 1/10 to 1/200 Hz. This error, however, is difficult to notice in view of the accuracy of the reaction enthalpy determination (±4%[5]).

Further extension of the frequency range is needed to explore the frequency effect in detail.[29] A frequency of 1/60 Hz was used in all the following isothermal and nonisothermal MTDSC experiments.

Nonisothermal cure. The effect of mixture composition on reaction rate is seen in the nonreversing (NR) heat flow during a nonisothermal cure experiment at 1°C/min [Fig. 10(a)]. The conversion as calculated from the NR heat flow was used to predict T_g as a function of temperature (T_g–x relation: see Fig. 2 and Table I). This calculated glass transition is plotted in Figure 10(b) for the stoichiometric (①) and excess amine (②) DGEBA + MDA mixture as a function of T_{cure}. The region above the dotted line corresponds to a material in the glassy state ($T_g > T_{cure}$), whereas the material is in the liquid or rubbery state below this line ($T_g < T_{cure}$).[20] Initially, the material is in the glassy state and devitrification of both unreacted mixtures occurred around −16°C (T_{g0}), as can also be seen in the heat capacity

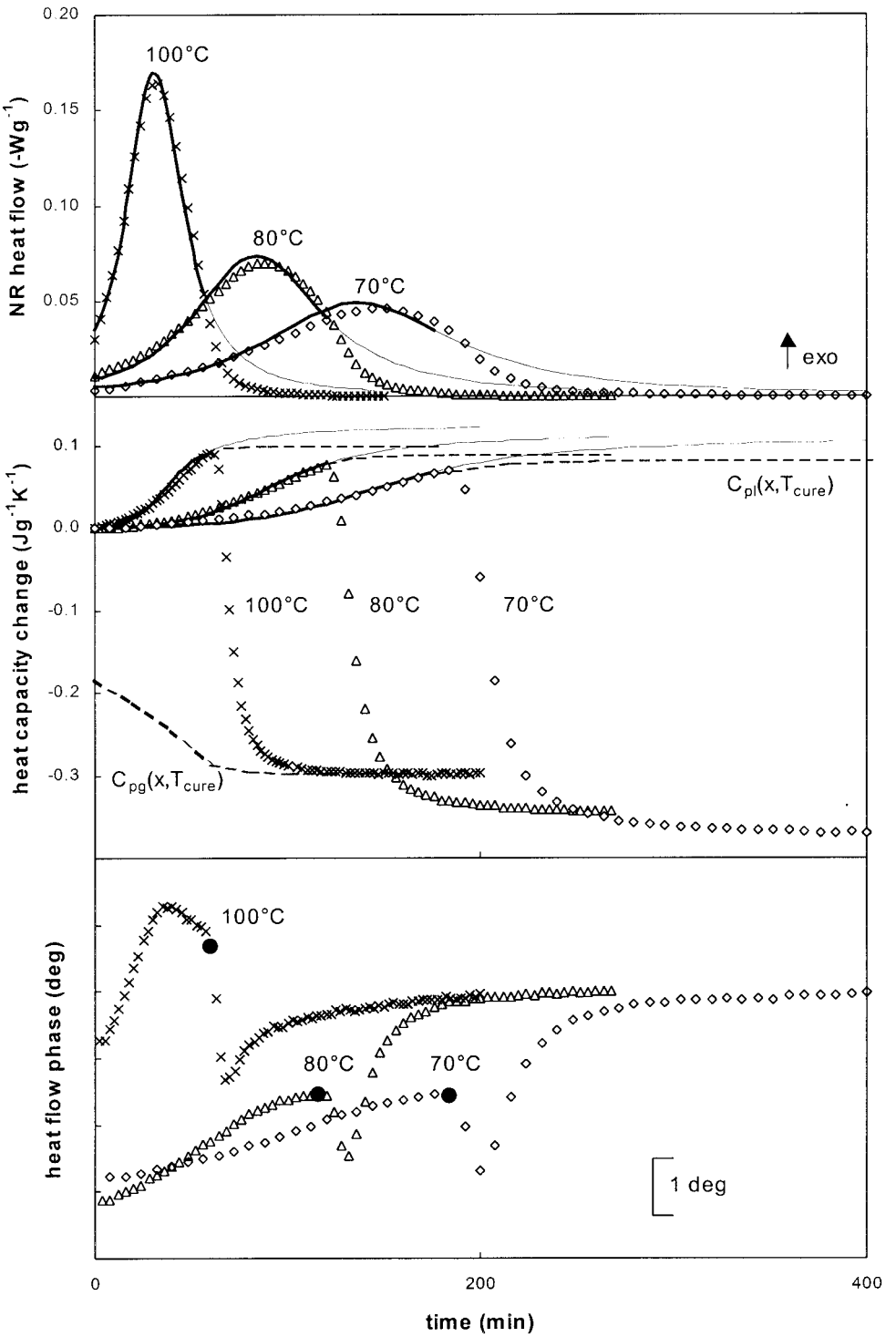

Figure 7 Nonreversing (NR) heat flow, heat capacity change (ΔC_p), and heat flow phase (ϕ) for the isothermal cure of stoichiometric DGEBA + MDA mixtures at 70 (◇), 80 (△), and 100°C (×); simulations of NR heat flow and ΔC_p for chemically controlled cure are depicted using the parameter set of Table III: a thick line is shown until the onset of vitrification as obtained from ϕ (indicated with ● in this signal); the contribution of the reaction heat capacity to ΔC_p in the diffusion-controlled region is also shown [$C_{pl}(x, T_{cure})$ in eq. (4), dashed line]; the glassy state reference heat capacity [$C_{pg}(x, T_{cure})$ in eq. (4), dashed line] is shown only for T_{cure} at 100°C for clarity.

signal [Fig. 10(c), 1st]. The reaction started around 50°C, where a slight increase in T_g was noticed. The steepest increase in T_g was seen at the maximum in the nonreversing heat flow, that is, at T_{cure} equal to 109 and 115°C for the excess amine and stoichiometric system, respectively. The earlier increase in T_g of the

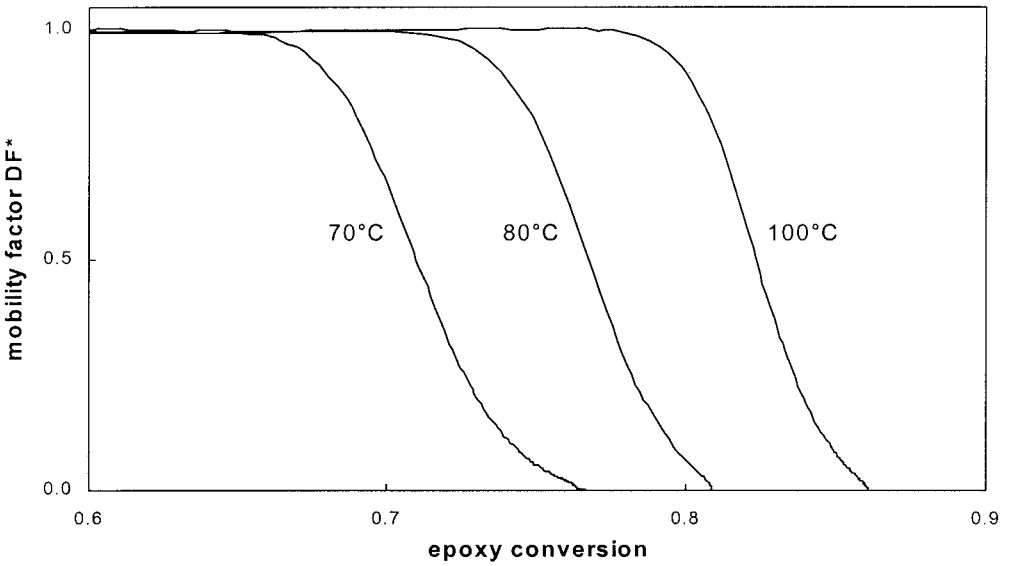

Figure 8 Mobility factor for modulation frequency f_M = 1/60 Hz (DF*) as a function of epoxy conversion for the isothermal cure of stoichiometric DGEBA + MDA mixtures at 70, 80, and 100°C.

former system resulted from its higher reaction rate as seen in the NR heat flow signal. Because the increase in T_g was much faster than the increase in T_{cure}, T_g increased above T_{cure}, which induced (partial) vitrification. This can be seen in the heat capacity signal as a stepwise decrease superimposed on the increase in C_p attributed to the reaction, starting at 117 and 129°C for r = 1.36 and r = 1, respectively [Fig. 10(c)].

The C_p increase attributed to the chemical reaction was also simulated with the kinetic parameters from Table III and corresponds to $C_{pl}(x, T)$ in eq (4). As a result of vitrification, the rate of reaction decreased rapidly, also resulting in a decrease of the rate with which T_g increases. A maximum difference $T_g - T_{cure}$ of 13°C was achieved. The C_p evolution with temperature in the fully vitrified state was calculated from extrapolation of the temperature dependency of the unreacted glassy material, whereas the effect of conversion was obtained from Figure 3. $C_{pg}(x, T)$ obtained in this way is also depicted in Figure 10(c) and represents C_p in the fully vitrified state. The experimental C_p evolutions never reach this state, which means that a

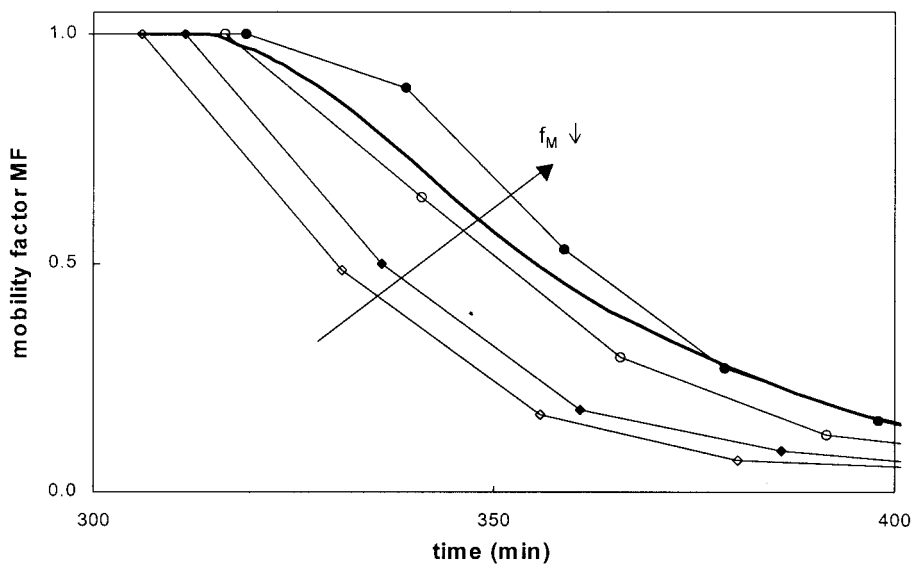

Figure 9 Mobility factor MF as a function of modulation frequency f_M for the isothermal cure of a stoichiometric DGEBA + MDA mixture at 60°C: 1/10 (◇), 1/20 (◆), 1/60 (○), and 1/200 Hz (●) are shown (thin lines); the diffusion factor DF was calculated from the ratio between the observed nonreversing heat flow and the calculated one in chemically controlled conditions (thick line).

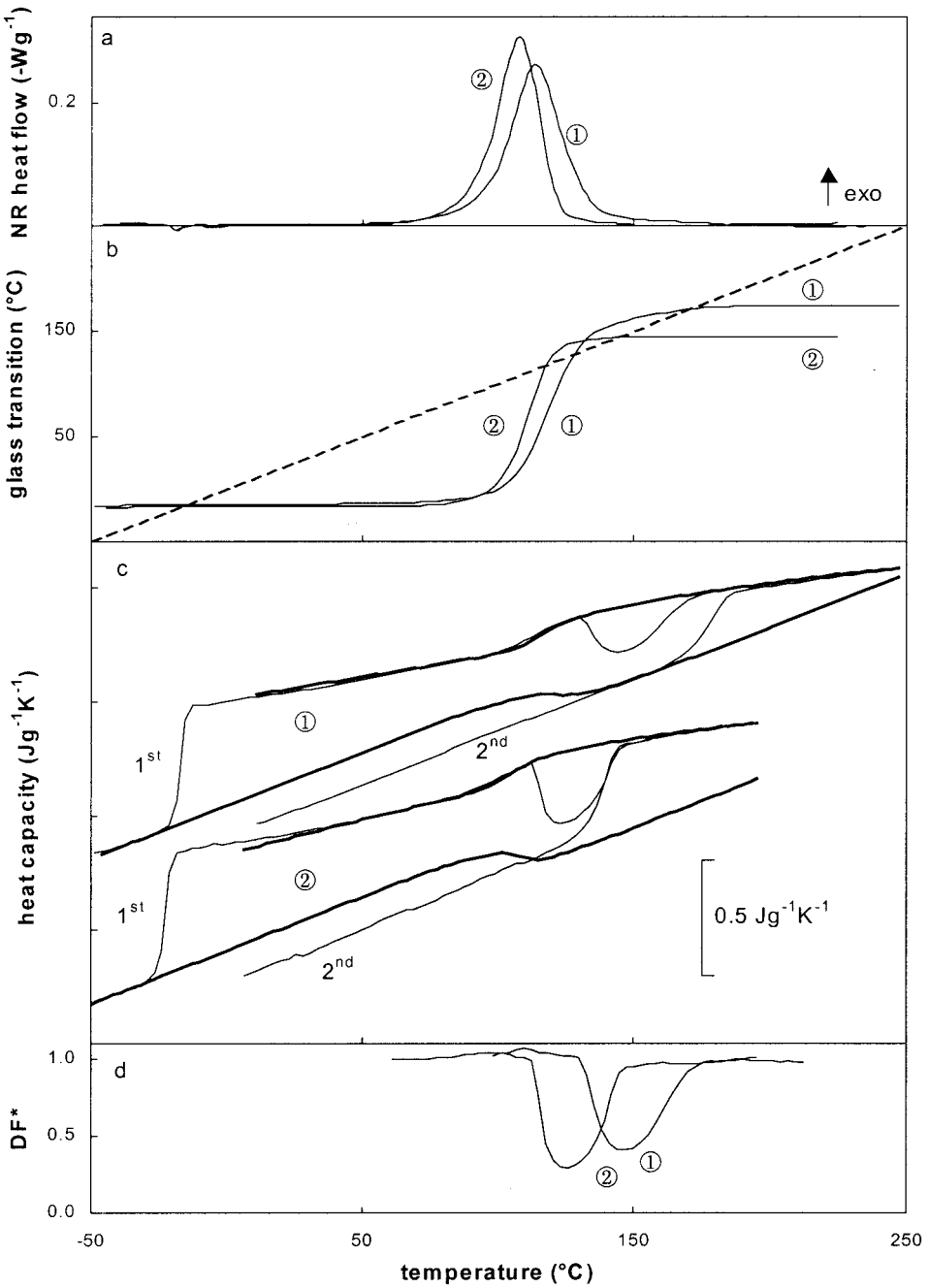

Figure 10 Nonisothermal cure at 1°C/min of a stoichiometric (r = 1, ①) and excess amine (r = 1.36, ②) DGEBA + MDA mixture: (a) nonreversing (NR) heat flow; (b) glass transition calculated from the conversion out of the NR heat flow and the T_g–x relationship [eq. (8)] (—), $T_g = T_{cure}$ (– – –); (c) heat capacity for a first (1st) and second heating (2nd) experiment (thin line); upper thick lines indicate $C_{pl}(x, T)$ as obtained from the simulation of chemically controlled cure and lower thick line indicate $C_{pg}(x, T)$ as obtained from extrapolating the temperature dependency of the C_p evolution in the glassy unreacted sample (1st) and the dependency of the C_p in the glassy state with conversion (see Fig. 3); (d) mobility factor (DF*) as calculated from the signals in (c) using eq. (4) and f_M = 1/60 Hz.

certain mobility will remain for both mixture compositions (partial vitrification). Because of the slower increase in T_g, devitrification occurred before T_{gfull} (175°C) in the stoichoimetric system, whereas the excess amine system devitrified at T_{gfull} (140°C) [Fig. 10(c), 2nd].

The mobility factor as calculated with eq. (4) from the experimental C_p evolutions and the reference liquid [$C_{pl}(x, T)$] and glassy [$C_{pg}(x, T)$] heat capacities is shown in Figure 10(d). Although the reaction is not completely inhibited in both systems, the excess amine mixture (Fig. 10, ②) shows a larger extent of mobility

TABLE IV
Optimized Set of Diffusion Parameters for the Stoichiometric (r = 1) and the Amine Excess DGEBA + MDA System (r = 1.36)[a]

r	ln A_D	E_D (kJ mol^{-1})	C_1	C_2 (°C)
1.0	17.8	59.9	5	64
1.36	10.1	50.3	11	60
1.36[b]	13.9	48.7	9	40

[a] A_D is the preexponential factor, E_D is the activation energy (kJ mol^{-1}), and C_1 and C_2 are constants from the WLF equation [see eq. (7)].
[b] Corresponds to the optimized parameter set when only DF* profiles are used from isothermal cure experiments.

restriction (minimum at DF* = 0.3) than that of the stoichiometric mixture (minimum at DF* = 0.4) attributed to its higher reaction rate. Using a lower heating rate or a highly reactive epoxy–amine system will result in more mobility restrictions in nonisothermal experiments.[20]

Finally note that for the excess epoxy mixture (r = 0.7), the nonisothermal cure at 1°C/min does not give rise to reaction-induced vitrification (not shown) because of the combined effect of a lower reaction rate and a lower $T_{g\text{full}}$ (90°C). Although isothermal cure below $T_{g\text{full}}$ can still result in diffusion-controlled reaction in these systems, the slow reaction and high conversion at the onset of vitrification result in unnoticeable changes in the heat flow signal. This can be compared to the situation of the DGEBA + aniline system ($T_{g\text{full}}$ = 95°C for r = 1).[15]

Optimized set of diffusion parameters

The evolution of DF* in both isothermal and nonisothermal conditions for the excess amine and stoichiometric system was used to obtain an optimized set of diffusion parameters (for cure conditions, see earlier section on optimized set of parameters for chemically controlled reactions). The kinetic parameters were fixed to the values obtained from the reaction in chemically controlled conditions (see Table III). With these parameters, the overall kinetic rate constant $k_{\text{kin}}(x, T)$ can be calculated [eq. (5)]. Although the T_g–x relations as obtained from Table I and eq. (8) were used without modification, all parameters of the diffusion rate constant k_D [A_D, E_D, C_1, and C_2 in eq. (7)] were optimized using the initial parameter set from Table II. In this way, the amount of fitting parameters can be reduced. The best fit of the diffusion factors DF [eq. (3)] to DF* is obtained with the parameters in Table IV. Subsequently, a refinement of the model was attempted by reoptimizing the kinetic parameters and the parameters from the T_g–x relationship [eq. (8)]. The results of this approach are not shown because no improvement on the least sum of squares could be obtained in this way.

Note, however, that in the case of the excess amine system, a better fit of the isothermal diffusion-controlled reaction can be found by limiting the optimization strategy to the isothermal DF* profiles (included in Table IV). This is illustrated in simulations in the next section.

Finally, note that the significant deviations between the optimized parameters (Table IV) and the initial parameter set (Table II) can be partly attributed to the fact that to obtain the latter set, the universal value of C_2 equal to 51.6°C was assumed.

Simulation capability

One should keep in mind that the kinetic parameter set from Table III together with the parameters for the diffusion model from Table IV are optimized for multiple experiments and mixture compositions, which results in a model that is valid for a wide range of conditions, but also in a somewhat lesser fit for the individual experiments.

Rate of reaction steps

By using the optimized parameter sets from both Table III and Table IV in combination with the T_g–x relation from Table I and eq. (8), the consumption rate of epoxide groups ($-d$[E]/dt) during the cure at 80°C of a stoichiometric DGEBA + MDA mixture can be calculated until the final conversion. A comparison is made with the DGEBA + aniline reaction at the same cure temperature in Figure 11. As was the case in the model epoxy–amine PGE + aniline,[14] the reaction of the primary amine with the epoxy–amine complex initiates reaction (corresponding to 2–4% conversion). Beyond this point, the epoxy–hydroxyl complex proves to be more reactive. The reactions of both amines with this complex are about twice as fast in the case of the MDA hardener compared to the aniline hardener. The higher reactivity of MDA toward DGEBA has been attributed to the inductive effect of the *para*-methylene group.[60] In contrast, vitrification inhibits the DGEBA + MDA reaction around 70% conversion.

Also note that for both systems, a competition between the primary amine and secondary amine for reaction with epoxy functionalities occurs from around 50% epoxy conversion. At higher conversions, the depletion of primary amine groups results in a predominance of the secondary amine–epoxy reaction.

Isothermal cure

The effect of mobility restrictions on the reaction rate is nicely simulated for the stoichiometric system at

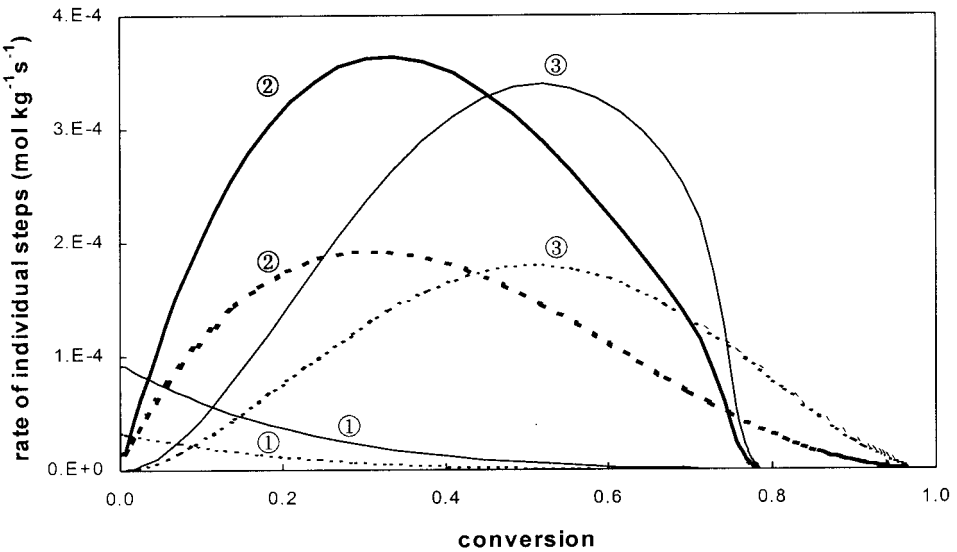

Figure 11 Consumption rate of epoxide groups ($-d[E]/dt$) at 80°C during the reaction of primary amine groups with the epoxy–amine complex (①); the reaction of the epoxy–hydroxyl complex with primary (②) and secondary (③) amine groups for the DGEBA + MDA system (lines) as simulated by using the parameter sets from Tables III and IV; the simulation for the DGEBA + aniline system by using the optimized parameters from Ref. 15 is also shown (dashed lines).

different cure temperatures (arrow in Fig. 12). This graph can be compared to Figure 7 where only the chemically controlled reaction was simulated. The simulated diffusion factors DF agree well with the experimental DF* profiles in Figure 13. Deviations occur both for high and low cure temperatures (100 and 50°C, respectively). A combination of the experimental error and the limited predictability of the temperature dependency of the diffusion rate constant k_D could be causing this discrepancy. Note that although the NR heat flow is not sensitive enough to measure the reaction rate in the case of the 50°C cure (not shown), DF* can still be determined accurately from the heat capacity signal (Fig. 13).

The effect of a change in mixture composition is simulated in Figure 14. A higher reaction rate was found when the concentration of amine groups was raised (from Fig. 14 compare ①, 100°C with ②, 100°C). Because no reaction-induced vitrification can occur for the system with an excess amount of epoxide groups

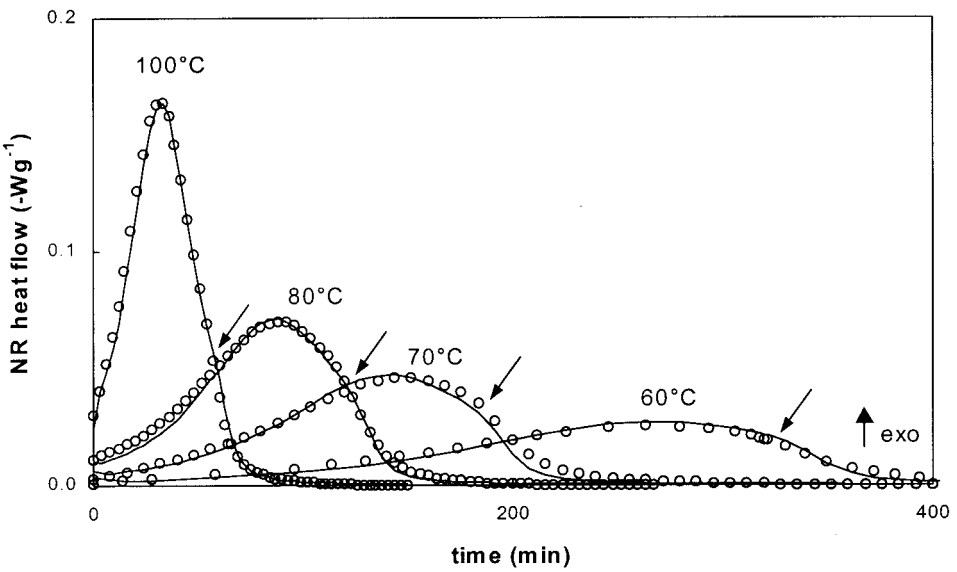

Figure 12 Nonreversing (NR) heat flow for the isothermal cure of stoichiometric DGEBA + MDA mixtures at 60, 70, 80, and 100°C (○); simulations using both the kinetic (Table III) and diffusion parameters (Table IV) (—); arrow indicates onset of diffusion control.

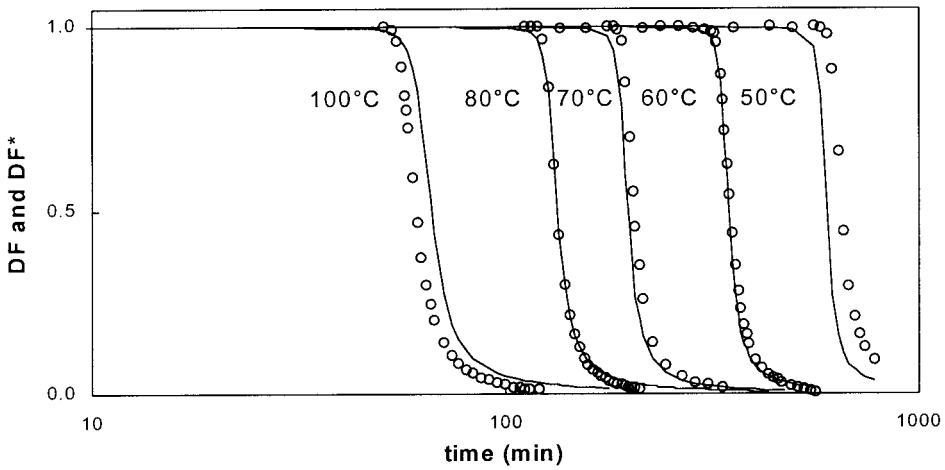

Figure 13 Experimental DF* (○) and simulated DF (—) for the isothermal cure of stoichiometric DGEBA + MDA mixtures at 50, 60, 70, 80, and 100°C.

(r = 0.7, ②: T_{gfull} = 91°C < T_{cure}), a symmetric heat flow signal was found, which can be compared to experiments on the DGEBA + aniline system in the first part of this series.[15] Further evidence of the absence of vitrification can be found in the heat capacity signal, given that only the change attributed to the reaction heat capacity is seen here (inset in Fig. 14). Note that the diffusion-controlled reaction for the excess amine system (Fig. 14, ①) is less well described for the lowest cure temperature. As can be seen more clearly from Figure 15, the diffusion factor decreases early compared to the experimental DF* profiles (note log scale in this figure). A closer fit can be obtained by optimizing the parameters for the diffusion rate solely from isothermal cure experiments. It turns out that the amount of vitrification in nonisothermal conditions [see, e.g., minimum in Fig. 10(d)] and the temperature at which devitrification occurs form the main basis for the difference in the optimized parameters.

Nonisothermal cure

The increase in reaction rate for higher amine concentrations is seen as a shift of the maximum heat flow to lower temperatures in nonisothermal conditions (Fig.

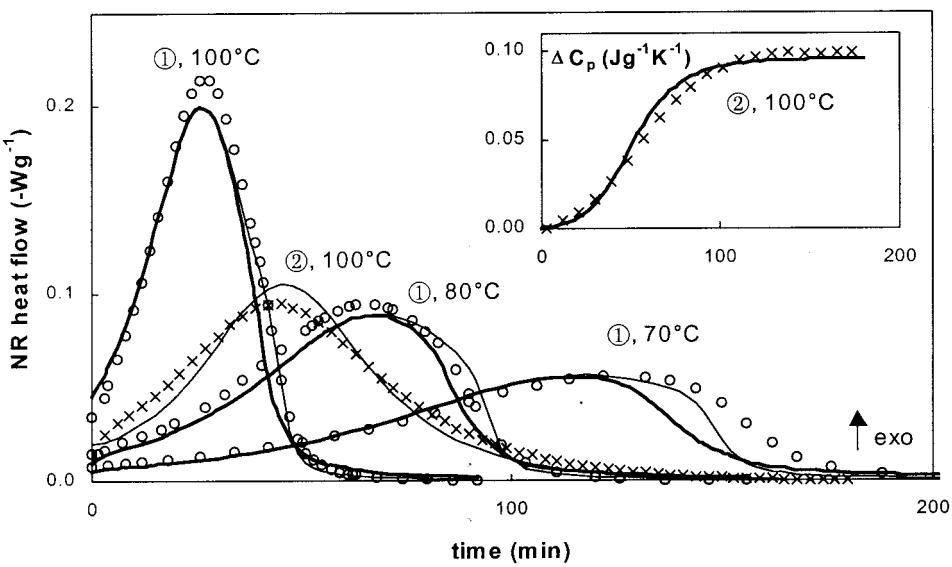

Figure 14 Nonreversing heat flow for the isothermal cure of DGEBA + MDA mixtures with an excess in amine groups (①, r = 1.36) at 70, 80, and 100°C (○) and an excess in epoxide groups (②, r = 0.7) at 100°C (×); simulations using both the kinetic (Table III) and diffusion parameters (Table IV) (thick line); the inset shows the experimental (×) and simulated (thick line) heat capacity change (ΔC_p) for the excess epoxy mixture at 100°C; simulations using diffusion parameters that were optimized for isothermal cure experiments only (Table IV) (thin line).

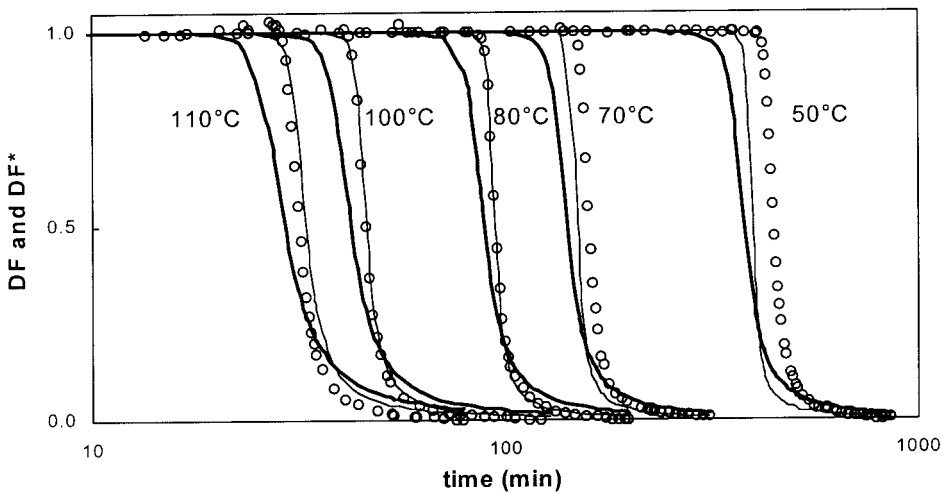

Figure 15 Experimental DF* (○) and simulated DF (thick line) for the isothermal cure of DGEBA + MDA mixtures with an excess in amine groups (r = 1.36) at 50, 70, 80, 100, and 110°C; simulations using diffusion parameters that were optimized for isothermal cure experiments only are also shown (Table IV) (thin line).

16). At 2.5°C/min, none of these mixtures shows vitrification because the rate of T_g increase is not sufficient to surpass the increase in T_{cure} (not shown).

The reaction-induced vitrification in nonisothermal conditions is illustrated in Figure 17 for lower heating rates in the case of the excess amine mixture. In this case, T_g increases up to the cure temperature and a mobility-restricted, retarded reaction occurs (see also Fig. 10). The lowest heating rate induces a more pronounced diffusion-controlled reaction. The dashed line simulates the heat flow in case no mobility restrictions would occur. Compared to the simulation including diffusion effects (continuous line), the decrease in reaction rate occurs a few degrees beyond the maximum reaction rate. In diffusion-controlled conditions, corresponding to the temperature range in the decrease of the diffusion (mobility) factor evolution, a low reaction rate remains, which is qualitatively predicted by the model. From a practical point of view, this shoulder should not be overlooked because it occurs over a temperature interval of about 35 and 20°C for the experiments at 0.5 and 1°C/min, respectively, and results in an additional T_g increase of up to 40°C.

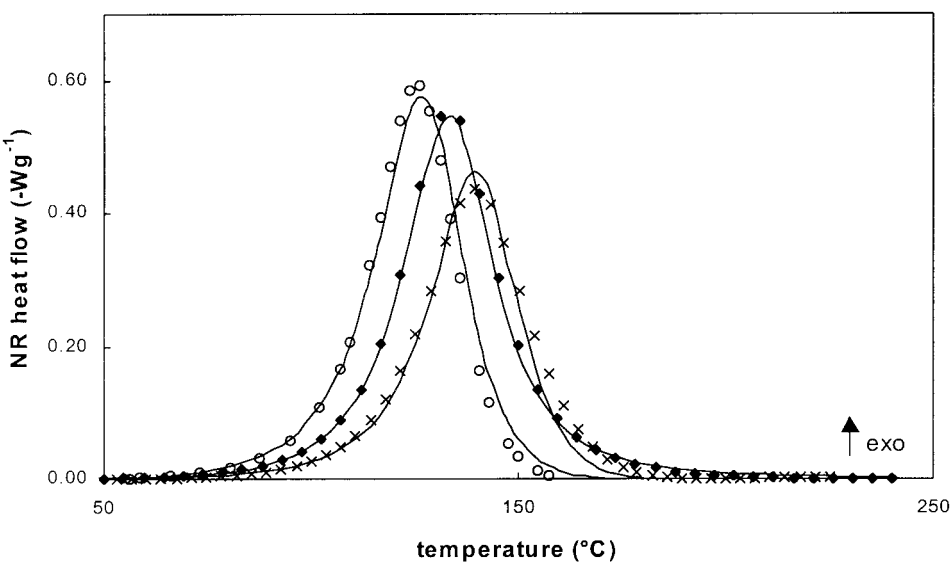

Figure 16 Nonreversing (NR) heat flow for the nonisothermal cure at 2.5°C/min of a stoichiometric (r = 1, ◆), excess amine (r = 1.36, ○), and excess epoxy (r = 0.7, ×) DGEBA + MDA mixture; simulations using both the kinetic (Table III) and diffusion parameters (Table IV) (—).

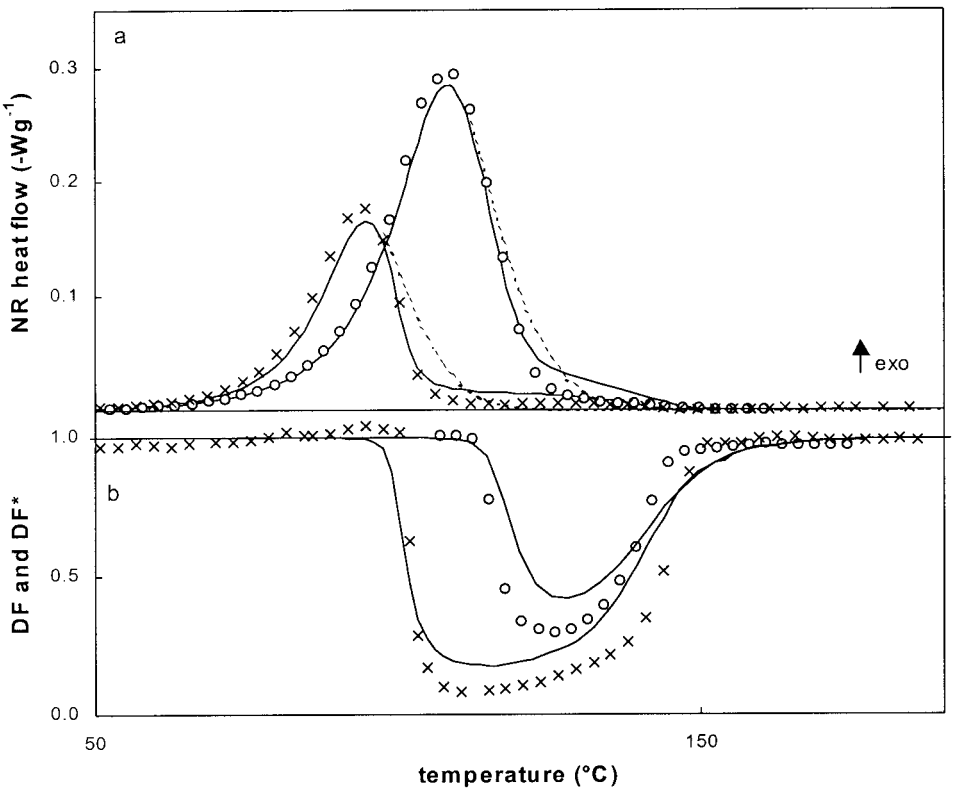

Figure 17 Nonreversing (NR) heat flow (a) and DF* (b) for the nonisothermal cure at 1°C/min (○) and 0.5°C/min (×) of an excess amine (r = 1.36) DGEBA + MDA mixture; simulations using both the kinetic (Table III) and diffusion parameters (Table IV) for the NR heat flow and DF are shown (—); simulated chemically controlled rate using only the kinetic parameters (– – –).

Combined isothermal and nonisothermal cure schedule

For curing large parts, the exothermic reaction can result in inferior mechanical properties if the rate of heat production is greater than the rate of heat dissipation.[1,61] The selection of low heating rates or combined cure paths can be useful in reducing internal stresses and can also be used to control reaction rates of highly exothermic reactions. The final cure temperature should be chosen above $T_{g\text{full}}$ to consume all reactive functionalities, while staying below the degradation onset. To test the capability of the model in practical conditions of complex cure schedules, Figure 18 depicts a partial isothermal cure at 100°C followed by a nonisothermal postcure at 2.5°C/min. Note that these conditions were used to develop the T_g–x relationships discussed earlier in the section on glass transition. Both cure stages are well predicted by the model. Interestingly, diffusion-controlled reaction occurs in the nonisothermal postcure at 2.5°C/min around 132 min corresponding to a temperature of 112°C. Note that no interference with vitrification was seen in the same nonisothermal cure of a fresh sample (Fig. 16). However, the isothermally pretreated sample has different concentrations of reactive groups (e.g., hydroxyl) at the start of the nonisothermal experiment, which is translated into a higher reaction rate and thus a faster increase in T_g, leading to partial vitrification.

CONCLUSIONS

The relationship between T_g and conversion is crucial to understand reaction-induced (partial) vitrification in both isothermal and nonisothermal conditions. The effect of a change in mixture composition on this relation can be predicted with the Couchman equation, requiring the T_g and the heat capacity change at T_g [$\Delta C_p(T_g)$] of the unreacted and fully reacted material. For an excess epoxy mixture, a correction to this equation is needed. In the fragility terminology, a net evolution to a stronger liquid is found from plots of $\Delta C_p(T_g)$ as a function of x. The full cure glass transition attains its maximum for a stoichiometric mixture, corresponding to the maximum in crosslink density for this composition.

Vitrification marks the onset of diffusion-controlled reaction during the step-growth polymerization of DGEBA + MDA. A model based on the Rabinowitch approach can be used to calculate the diffusion factor DF, which reflects whether the overall kinetic rate constant (k_{kin}) or the overall diffusion rate constant

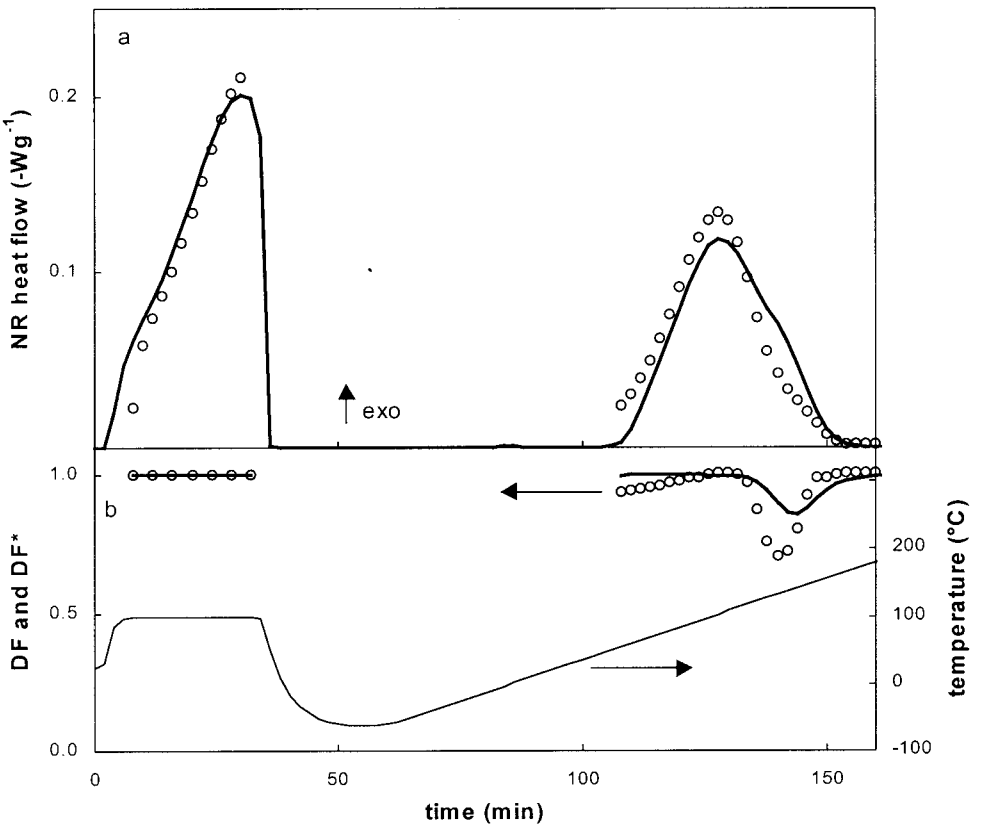

Figure 18 Nonreversing (NR) heat flow (○, a) and DF* (○, b) for the combined cure schedule consisting of an isothermal cure at 100°C (22 min) follows by a fast quench and subsequently a nonisothermal postcure at 2.5 °C/min (thin line, b); simulations using both the kinetic (Table III) and diffusion parameters (Table IV) for the NR heat flow and DF (thick line).

(k_D) determines the rate during cure. k_D can be obtained by using a description similar to the Williams–Landel–Ferry equation based on free volume concepts, together with an Arrhenius temperature dependency. Describing both the effect of cure temperature (T_{cure}) and mixture composition (r) on the reaction rate requires a mechanistic approach, which includes the elementary amine–epoxy reaction steps together with equilibrium complexes between the epoxy, amine, hydroxyl, and ether groups in the reactive mixture.

To optimize the kinetic and diffusion parameters of the presented model, experimental input is provided by the nonreversing heat flow and the heat capacity from MTDSC in both isothermal and nonisothermal conditions for different mixture compositions. Both signals contain complementary information about the chemical reaction. The mobility factor MF, as obtained from the stepwise decrease in the heat capacity signal, describes the amount of mobility restriction and vitrification. To ensure that MF contains only the effect of a change in segmental mobility, the contribution from the reaction heat capacity must be taken into account. Moreover, the evolution of C_p with temperature and conversion in the fully vitrified state is required as a reference for complete mobility inhibition. An increase in the modulation frequency decreases the vitrification time, thus changing MF, whereas DF depends only on the underlying temperature. For the standard frequency (1/60 Hz) used in MTDSC, the mobility factor MF(1/60 Hz) = DF* turns out to be close to DF, indicating that the segmental mobility frozen in at T_g in these conditions corresponds to the rate-determining mobility upon transition to diffusion-controlled reaction conditions. DF* can thus be used as a model for DF.

The presented model with the optimized set of kinetic and diffusion parameters is able to predict changes in reaction rate with T_{cure} and r in both chemically controlled and diffusion-controlled conditions. Apart from isothermal and nonisothermal cure, a combined cure path, of interest in practical applications, can also be simulated. In this way, an optimum cure schedule can be developed, which reduces the cure time, but ensures a uniform temperature gradient in the sample.

The mechanistic approach allows for further extension so that the effect of (reactive) additives could also be included, either by adding reaction steps or by including additional equilibrium complexes accounting for physical interactions. It further allows attribution of a specific correction to the "overall" diffusion factor DF for each reaction step of the mechanistic

model. In this way, it could be investigated whether the concept of overall diffusion control is too rough an approximation for the step-growth epoxy–amine cure and a more balanced "specific" diffusion control is preferable.

The work of S. Swier was supported by grants of the Flemish Institute for the Promotion of Scientific-Technological Research in Industry (I.W.T.). G. Van Assche is a postdoctoral researcher of the Foundation for Scientific Research FWO—Flanders (Belgium).

References

1. Gillham, J. K.; Enns, J. B. Trends Polym Sci 1994, 2, 406.
2. Young, R. J.; Lovell, P. A. Introduction to Polymers; Chapman & Hall: London, 1991; Chapter 2.
3. Dusek, K.; Havlisek, I. Prog Org Coat 1993, 22, 145.
4. Stutz, H.; Mertes, J.; Nuebecker, K. J Polym Sci Part A: Polym Chem 1993, 31, 1879.
5. Swier, S.; Van Mele, B. J Polym Sci Part B: Polym Phys 2003, 41, 594.
6. Horie, K.; Mita, I. Adv Polym Sci 1989, 88, 77.
7. Rabinowitch, E. Trans Faraday Soc 1937, 33, 1225.
8. Van Assche, G.; Swier, S.; Van Mele, B. Thermochim Acta 2002, 388, 327.
9. Deng, Y.; Martin, G. C. Macromolecules 1994, 27, 5147.
10. Horie, K.; Hiura, H.; Sawada, M.; Mita, I.; Kambe, H. J Polym Sci Part A1: Polym Chem 1970, 8, 1357.
11. Kamal, M. R. Polym Eng Sci 1974, 14, 231.
12. Cole, K. C. Macromolecules 1991, 24, 3093.
13. Dupuy, J.; Leroy, E.; Maazouz, A. J Appl Polym Sci 2000, 78, 2262.
14. Swier, S.; Van Mele, B. Thermochim Acta, to appear.
15. Swier, S.; Van Assche, G.; Van Mele, B. J Appl Polym Sci 2004, 91, 2798.
16. Finzel, M. C.; Delong, J.; Hawley, M. C. J Polym Sci Part A: Polym Chem 1995, 33, 673.
17. Chern, C. S.; Poehlein, G. W. Polym Eng Sci 1987, 27, 788.
18. Girard-Reydet, E.; Riccardi, C. C.; Sautereau, H.; Pascault, J. P. Macromolecules 1995, 28, 7599.
19. Van Assche, G.; Van Hemelrijck, A.; Rahier, H.; Van Mele, B. Thermochim Acta 1995, 268, 121.
20. Van Assche, G.; Van Hemelrijck, A.; Rahier, H.; Van Mele, B. Thermochim Acta 1996, 286, 209.
21. Van Assche, G.; Van Hemelrijck, A.; Rahier, H.; Van Mele, B. Thermochim Acta 1997, 304/305, 317.
22. Montserrat, S.; Cima, I. Thermochim Acta 1999, 330, 189.
23. Lange, J.; Altmann, N.; Kelly, C. T.; Halley, P. J. Polymer 2000, 41, 5949.
24. Nass, K. A.; Seferis, J. C. Polym Eng Sci 1989, 29, 315.
25. Senturia, A. D.; Sheppard, N. F. Adv Polym Sci 1986, 80, 1.
26. Malkin, A. Y.; Kulichikhin, S. G. Adv Polym Sci 1991, 101, 217.
27. Shaw, S. J. In: Chemistry and Technology of Epoxy Resins; Ellis, B., Ed.; Blackie Academic and Professional: London, 1994; Chapters 4 and 7.
28. Schawe, J. E. K. J Therm Anal Calorim 2001, 64, 599.
29. Van Assche, G.; Van Mele, B.; Saruyama, Y. Thermochim Acta 2001, 377, 125.
30. Swier, S.; Van Assche, G.; Van Hemelrijck, A.; Rahier, H.; Verdonck, E.; Van Mele, B. J Therm Anal Calorim 1998, 54, 585.
31. Van Assche, G.; Verdonck, E.; Van Mele, B. Polymer 2001, 42, 2959.
32. Shell Method HC-427-81: Perchloric acid method.
33. Gaur, U.; Wunderlich, B. J Phys Chem Ref Data 1982, 11, 313.
34. Cassel, R. B. TA Instruments Applications Brief TA 282; TA Instruments: New Castle, DE.
35. Danley, R. L.; Caulfield, P. A. In: Proceedings of the 29th Conference of the North American Thermal Analysis Society, TA Instruments Applications Brief TA 268; TA Instruments: New Castle, DE, 2001; pp. 667–672.
36. Deng, Y.; Martin, G. C. Macromolecules 1994, 27, 5141.
37. Williams, M. L.; Landel, R. F.; Ferry, D. J. J Am Chem Soc 1955, 77, 3701.
38. Mark, J. E. In: Physical Properties of Polymers Handbook, Part V. 25; Larson, R.; Pincus, P. A., Eds.; American Institute of Physics: New York, 1996.
39. Gerard, J. F.; Galy, J.; Pascault, J. P. Polym Eng Sci 1991, 31, 615.
40. Aronhime, M. T.; Gillham, J. K. J Coat Technol 1984, 56, 35.
41. Hale, A.; Macosko, C. W.; Bair, H. E. Macromolecules 1991, 24, 2610.
42. Simon, S. L.; Gillham, J. K. J Appl Polym Sci 1994, 53, 709.
43. Wang, X.; Gillham, J. K. J Appl Polym Sci 1992, 45, 2127.
44. Couchman, P. R.; Karasz, F. E. Macromolecules 1978, 11, 117.
45. Venditti, R. A.; Gillham, J. K. J Appl Polym Sci 1997, 64, 3.
46. Rozenberg, B. A. Adv Polym Sci 1986, 75, 113.
47. Kamon, T.; Furukawa, H. Adv Polym Sci 1986, 80, 173.
48. Oleinik, E. F. Adv Polym Sci 1986, 80, 49.
49. Vallo, C. I.; Frontini, P. M.; Williams, R. J. J. J Polym Sci Part B: Polym Phys 1991, 29, 1503.
50. Cole, K. C. Macromolecules 1991, 24, 3093.
51. Wisanrakkit, G.; Gillham, J. K. J Coat Technol 1990, 62, 35.
52. Halary, J. L. High Perform Polym 2000, 2, 141.
53. Montserrat, S. Polymer 1995, 36, 435.
54. Cook, W. D.; Mehrabi, M.; Edward, G. H. Polymer 1999, 40, 1209.
55. Wang, X. J Appl Polym Sci 1997, 64, 69.
56. Angell, C. A. J Res Natl Inst Stand Technol 1997, 102, 171.
57. Van Hemelrijck, A. Ph.D. Thesis, Free University of Brussels, Belgium, 1996.
58. Van Mele, B.; Rahier, H.; Van Assche, G.; Swier, S. In: The Application of MTDSC for the Characterization of Curing Systems: The Characterization of Polymers Using Advanced Calorimetric Methods; Reading, M., Ed.; Kluwer Academic: Dordrecht, to appear.
59. Barton, J. M. Adv Polym Sci 1985, 72, 111.
60. Mayr, A. E.; Cook, W. D.; Edward, G. H. Polymer 1998, 39, 3719.
61. Wisanrakkit, G.; Gillham, J. K.; Enns, J. B. J Appl Polym Sci 1990, 41, 1895.